Report to DRBC on concentrations of nutrients and chlorophyll a and rates of respiration and primary production in samples from Delaware Bay collected in May and July 2014

Thomas R. Fisher
Professor

Anne B. Gustafson
Senior Faculty Research Assistant

Horn Point Laboratory
Center for Environmental Science
University of Maryland
2020 Horn Point Road
Cambridge MD 21613

 NOTE: This version of the report contains corrected statistics in Tables 3A and 3B.

Report revised: 25 Jan 2019 trf

ERRATA SHEET

This errata sheet lists errors and their corrections for the document titled "Report to DRBC on concentrations of nutrients and chlorophyll a and rates of respiration and primary production in samples from Delaware Bay collected in May and July 2014" by Thomas R. Fisher and Anne. B Gustafson, University of Maryland Center for Environmental Science, 2015.

Location	Error	Correction
Table 3A	Incorrect summary statistics at bottom of table	Summary statistics corrected
Table 3B	Incorrect summary statistics at bottom of table	Summary statistics corrected

Introduction

In December 2012, the Delaware River Basin Commission (DRBC) convened a Modeling Expert Panel to initiate work on development of an Eutrophication model of the Delaware Estuary. This model was envisioned as a needed step toward the development of updated water quality criteria for dissolved oxygen and numeric nutrient criteria for the estuary, as described in DRBC's Nutrient Criteria Development Plan (http://www.nj.gov/drbc/library/documents/nutrients/del-river-estuary_nutrient-plan_dec2013.pdf). The Expert Panel reviewed existing information with DRBC and recommended among other activities the collection of new primary productivity data in the estuary. The effort described in this report reflects an initial response to the Expert Panel recommendation.

Sampling was conducted on two dates in 2014. On May 19, 2014 and July 21, 2014, DRBC staff collected surface water samples along three transects at River Miles 10, 25, and 40, with five sample sites on each transect for a total of 15 sample sites (Figure 1). An additional surface water sample was collected on each day from the Estuarine Turbidity Maximum (ETM) near River Mile 55. At each of the 15 sites, surface and bottom measurements of salinity, temperature, and dissolved oxygen (DO) were made. At sites where the difference between top and bottom salinity was greater than 1 (as indicated by the conductivity meter), or the difference between top and bottom DO was greater than 1 mg/L, a near bottom water sample was collected in addition to the near surface samples.   At each of the 15 transect sites, DRBC also measured photosynthetically active radiation (PAR) above the water and at one meter below the water surface.

Methods

Field data were collected by DRBC personnel *in situ*. Salinity, temperature, and dissolved oxygen (DO) data at the surface and bottom were obtained using a Measurement Specialties Eureka 3 water quality meter. Light extinction measurements were made using a LiCor LI-1400 data logger connected to a LI-190 surface PAR sensor and a LI-192 underwater sensor. Both sensors had been recently calibrated by LiCor on March 14, 2014. At each station, surface irradiance (I_O, $\mu E\ m^{-2}\ s^{-1}$) was measured simultaneously with irradiance at a depth z = 1 m (I_Z, $\mu E\ m^{-2}\ s^{-1}$). The light extinction coefficient in the water column (k, m^{-1}) was estimated from these two numbers as follows:

$$k = \ln(I_O/I_Z)/z = \ln(I_O/I_Z) \hspace{3cm} \text{eq. 1}$$

for z = 1 m. These measurements were made *in situ* on the vessel when the water samples were taken for subsequent analysis of nutrients, respiration, and primary production in our laboratory.

Water samples were collected at 16 stations (May: 16 surface samples, 7 bottom samples; July: 16 surface samples, 8 bottom samples) as described in the introduction by DRBC personnel on a vessel provided by Delaware Bay Launch Services. Collected water samples were maintained at ambient bay water temperature at 60% light (surface samples) or in darkness (bottom water samples) while on the ship. At the dock the samples were transferred late in the day to coolers to maintain bay water temperature as much as possible, and the samples were then driven to HPL. Within 1.5 h of the ship's arrival, the samples were transferred to a BOD box at the Horn Point Laboratory (HPL) maintained at 17.6∘C in May and 24.8∘C in July to approximate the median bay temperatures (17.8∘C in May, 25.2∘C in July). Lights within the box provided ~100 $\mu E\ m^{-2}\ s^{-1}$ of PAR on the appropriate day/night cycle for the month. Bottom samples were wrapped in black bags to maintain darkness. On the morning following sample collection, aliquots of the samples were placed in incubation bottles for measurements of respiration (all samples) and ^{14}C-based primary production (surface samples only). Details are provided below.

Samples for nutrient (NH$_4$, NO$_2$+NO$_3$, and PO$_4$, µM = µmoles L^{-1} = mmoles m^{-3}) and chlorophyll a (chla, µg L^{-1} = mg m^{-3}) analyses were filtered following the start of the incubations. Filtered samples were frozen at -5∘C and analyzed for nutrients within two weeks by automated colorimetry on a Technicon 2 AutoAnalyzer in the HPL Analytical Services Laboratory following the protocols of Lane et al (2000). The protocols followed EPA standard methods 350.1 for NH$_4$, 353.2 for NO$_3$ + NO$_2$, and 365.1 for PO$_4$ (soluble reactive phosphate). Filters for chla analysis were frozen and stored at -80∘C until analysis by fluorometry on a Turner Designs model 10-AU in the HPL Analytical Services Laboratory, generally within 2 months. The chla protocol followed the EPA 445.0 standard method.

Respiration was measured as the difference in oxygen concentrations (O$_2$, mg O$_2$ L^{-1}) between an initial measurement and a final measurement ~24 hour later. Initial and final samples were put into quadruplicate, 150 ml, darkened, BOD bottles with glass stoppers to exclude air contact. The initial samples were processed in sequence within hours as described below, and the remaining bottles were transferred to an incubator floating in the HPL boat basin subject to Choptank River temperatures and weak wave action. Final samples were returned to the lab ~24 hours later and were also analyzed in sequence for O$_2$ on the same day. All of the respiration samples were analyzed for O$_2$ by Membrane Inlet Mass Spectrometry (MIMS, Kana et al. 1994) with a precision of <0.5%. The first replicate of each set of four for each sample was used to condition the MIMS, and the remaining three were averaged for DO. MIMS simultaneously measures dissolved N$_2$, O$_2$, and Ar with high precision, and the ratios of N$_2$ and O$_2$ to Ar can be used to assess saturation relative to air equilibrium. The difference between the initial and final DO (DO$_i$, DO$_f$, mg O$_2$ L^{-1}) was used to calculate Respiration (R, mg O$_2$ L^{-1} d^{-1}, equivalent to g O$_2$ m^{-3} d^{-1}), as follows:

$$R = (DO_f - DO_i)/\Delta t \hspace{4cm} \text{eq. 2}$$

where Δt = time in days calculated from the average time of initial and final analyses for each station. Since DO$_i$ was always greater than DO$_f$, R is always negative, representing consumption of O$_2$.

Primary production measurements were performed on the samples stored overnight in the BOD box maintained at an appropriate diel light regime (described above). Six aliquots of sample (148 ml) were transferred to rinsed, transparent, 150 ml bottles. We added 0.1 ml of a ^{14}C-NaHCO$_3$ solution (1 μCi/ml activity) to each bottle, capped each bottle, mixed thoroughly, and filtered one of the bottles immediately to correct for particulate contaminants in the stock and ^{14}C sorption on particulates in the original water sample. The other five bottles were transferred into screened bags of varying thicknesses to attenuate the light to 60%, 32%, 15%, 7.5%, and 3.0% of surface Photosynthetically Active Radiation (PAR, 400-700 nm, E m^{-2} d^{-1}), which was monitored on the roof of HPL and calculated as described in Fisher et al. (2003). The bottles in their screens were then quickly transferred to the floating incubator described above, and incubated for ~24 hours, when they were returned to the laboratory for filtration. Following filtration on 25 mm GFF filters at <200 mm Hg vacuum, all filters (including the edges under the filter funnel) were rinsed with filtered sample water from the original sample to remove dissolved ^{14}C and then transferred to 7 ml scintillation vials with 3 ml of Ecoscint A fluor. Total ^{14}C activity (TA, dpm/ml) was measured using the addition of 0.1 ml of the ^{14}C stock or by addition of 1 ml of the spiked water sample to Ecoscint A fluor. All scintillation vials were allowed to sit for 24 hours in the Packard Tricarb model 2200CA liquid scintillation counter to eliminate auto-fluorescence from ambient light, and then counted to 1% counting accuracy. Total CO$_2$ (TCO$_2$ = sum of CO$_2$, H$_2$CO$_3$, HCO$_3^-$, and CO$_3^{-2}$) was calculated using the relationship of carbonate alkalinity to salinity reported for Delaware Bay by Sharp (2013). Primary production at simulated depth z (P$_z$, mg C L^{-1} d^{-1} = g C m^{-3} d^{-1}) was calculated as follows:

$$P_z = 1.05 * TCO_2 * (DPM_f - DPM_i) / (TA * \Delta t) \qquad \text{eq. 3}$$

where 1.05 corrects for the isotopic discrimination for ^{14}C-CO$_2$ uptake compared to ^{12}C-CO$_2$ uptake, DPM$_f$ and DPM$_i$ are the ^{14}C activity of the final and initial samples for each light level, and Δt is the time interval in days (approximately 1 day).

In general, we adhered to the protocols of Sharp et al. (2009) and Sharp (2013) for primary production measurements to maintain continuity with existing primary production datasets. Deviations from Sharp's protocols included: (1) lower ^{14}C activity added to our samples (0.1 µCi in 150 ml bottles vs 1 µCi in 80 ml bottles by Sharp), and (2) our attenuation screens were virtually identical to those used by Sharp, but we used a 3% compared to a 1.5% PAR level for the highest light attenuation (lowest light level). Neither of these deviations should have any significant effect on the rates of primary production at a given depth (P_z, g C m^{-3} d^{-1}) or integrated primary productivity (P, g C m^{-2} d^{-1}) reported here for comparison with Sharp's previous datasets.

We used the hyperbolic tangent model of Jassby and Platt (1976) to evaluate the effect of PAR on rates of primary production at any depth z (m) as (P_z):

$$P_z = P_m * \tanh(x)$$
<div align="right">eq. 4</div>

where P_m is the maximum, light-saturated primary production (g C m^{-3} d^{-1}). P_m is the asymptote as P_z approaches saturation, and x is a composite parameter defined as follows:

$$x = \alpha * PAR / P_m$$
<div align="right">eq. 5</div>

where α is the light-dependent primary productivity parameter (initial slope of P_z vs PAR with units of g C m^{-3} (E m^{-2})$^{-1}$. Values of P_z for each station at varying PAR were fit with the hyperbolic tangent function to obtain α and P_m. This equation is equivalent to models 1 (linear) and 2 (hyperbolic saturation) used by Sharp (2013). In the two datasets reported here for May and July in Delaware Bay, we saw no evidence of light inhibition (Sharp's model 3).

For ease of fitting the hyperbolic tangent (tanh) function to the P_z vs PAR data in SigmaPlot v12.5, we used the following transformation:

$$\tanh(x) = (e^{2x} - 1)/(e^{2x} + 1)$$
<div align="right">eq. 6</div>

which was obtained from:

http://www.roperld.com/science/Mathematics/HyperbolicTangentWorld.htm

In our application, we used the following formulation:

$$P_Z = P_m * (e^{2*\alpha*PAR/Pm} -1)/(e^{2*\alpha*PAR/Pm} +1) \qquad\qquad\qquad eq.7$$

where e is the exponential function, and all other parameters are described above. The hyperbolic tangent function fit the data well (r^2 generally > 0.90, see Fig. 2A, Tables 1 and 2)), and we were able to estimate α, the light-dependent primary production parameter (g C m^{-3} (E m^{-2})$^{-1}$) for every station. However, for seven of the May samples the relationship between P and PAR was essentially linear (Sharp's model 1), which enabled us to obtain α, but which prevented us from estimating P_m, the light-saturated primary production parameter (g C m^{-3} h^{-1}), which is independent of PAR. For consistency, we used eq. 7 to calculate α for all stations, but for seven May stations P_m was indeterminate.

We estimated integrated water column primary productivity (P, g C m^{-2} d^{-1}) using the measured water column extinction coefficient (k, m^{-1}, eq. 1) and the observed values of C fixation (P_Z) at the fixed light depths of 3-60%. Using k, we converted the light depth into water depth (z, m):

$$z = \ln(I_O/I_Z)/k \qquad\qquad\qquad eq. 8$$

where I_O is the total PAR (E m^{-2} d^{-1}) during the incubations and I_Z is the calculated irradiance at the light depth (E m^{-2} d^{-1}) based on the station k. I_O was obtained using a LiCor- 190 surface probe on the roof of a building at Horn Point attached to a LI-1000 data logger (see Fisher et al. 2003) integrated at hourly intervals (May: 35.13 E m^{-2} d^{-1}, July: 34.15 E m^{-2} d^{-1}). We extrapolated the observed volumetric C fixation rate at each depth to the midpoint between each depth above and below (Δz, m), except that the production at 60% light was extrapolated to the surface and the production at 3% light was extrapolated to one additional depth increment below the estimated value (see Fig. 2B). P was estimated as:

$$P = \Sigma (Pz*\Delta z) \qquad\qquad\qquad eq. 9$$

See Fig. 2B for an example.

All statistical analyses were done in SigmaPlot v12.5 and Excel 2010. The significance level for statistical tests was set at $p < 0.05$ (significant) or $p < 0.01$ (highly significant), unless otherwise noted.

When terms with errors were combined in a formula, propagation of error for the final result was based

on error in the individual components using the standard error propagation formulas in Bevington

(1969), assuming no error covariance. Parametric statistical comparisons and tests were done if the

data were normally distributed; otherwise an equivalent non-parametric test was used.

Results and Discussion

<u>Nutrients</u>

Concentrations of dissolved nutrients were generally high on both cruises (Tables 1 and 2).

Ammonium ranged over 0.3 - 8 µM on both cruises, averaging 2.4 ± 0.4 in May and 2.2 ± 0.6 in July, with

no significant differences between surface and bottom water on each cruise or between cruises. Nitrate

was more abundant than ammonium, ranging over 0.3 - 114 µM on both cruises and averaging 37 ± 7 in

May and 35 ± 7 in July. As for ammonium, there were no significant differences between surface and

bottom waters or between cruises. Phosphate had the lowest concentrations of the three major

nutrients, ranging over 0.07- 2 µM on both cruises and averaging 0.5 ± 0.1 in May and 1.2 ± 0.2 in July.

The average phosphate was twice as high in July compared to May, but the ranges for phosphate largely

overlapped. However, a paired t-test for the 23 overlapping stations showed that there was a significant

difference between the two groups (July > May, $p<0.01$).

Most of the concentrations reported in Tables 1 and 2 are considered saturating for

phytoplankton growth in estuaries (Fisher et al. 1995, 1999). The exceptions for nitrogen are top

stations RM10-04, RM10-05, RM10-06, RM10-07, and bottom station RM 25-06 in May, and top stations

RM10-02, RM 10-03, and RM10-04 in June. At these stations the dissolved inorganic N (NH_4 + NO_3) was

<2 µM, concentrations associated with N limitation in estuarine and coastal waters (Fisher et al. 1995).

The exceptions for phosphorus were top station RM25-10 in May and RM10-04 and RM10-05 in July. At

these stations the phosphate was <0.10 µM, concentrations associated with P limitation in estuarine

and coastal waters (Fisher et al. 1995). For the remainder of the stations (76%), both DIN and phosphate

were sufficiently abundant that it is likely that light and not nutrients were limiting phytoplankton

growth rates.

Nutrient concentrations exhibited varied behavior in mixing plots (Fig. 3). The distribution of

nitrate on the salinity gradient (top panel) was nearly linear, but the mixing lines intersected the x axis at

salinities of 22-26, implying nearly complete consumption of nitrate within the estuary. In addition, there was clearly some non-conservative behavior with very low nitrate concentrations at salinities of 20-30, indicating local depletion of nitrate at higher salinities in the lower bay. Ammonium showed no systematic patterns with respect to salinity (Fig. 3, middle panel), but many of the values >4 µM occurred in bottom waters. However, the highest value of ammonium was in surface waters at RM10-01. This pattern is consistent with coupled uptake and regeneration of ammonium within the estuary, with a slight excess of regeneration in the water column and sediments leading to small accumulations of ammonium in the water column (0.2-8 µM). The distribution of phosphate on the salinity gradient exhibited sigmoidal behavior, with values >1 µM associated with lower salinities (<10 in May, <20 in July). These distributions of nitrate and phosphate on the salinity gradient are reverse images of the behavior of chlorophyll a on the salinity gradient caused by the inverse relationships of chlorophyll *a* with nitrate and phosphate (next section, see Fig. 4). Note that the interpretation of the data in Fig. 3 is limited by incomplete transects of the salinity gradient, resulting in weak definitions of the fresh and coastal end members, which limits the interpretation of the mixing patterns.

Chlorophyll *a*

Phytoplankton biomass, as indicated by chlorophyll *a* concentrations, varied over large ranges on the two cruises (Tables 1 and 2). Chlorophyll *a* ranged over 4-108 µg L^{-1} in May and 2-61 µg L^{-1} in July, averaging 29 ± 2 in May and 17 ± 1 in July. A Wilcoxon signed-rank test of paired stations indicated that May chlorophyll *a* values were systematically higher than those in July ($p<0.01$). These high values of chlorophyll *a* are indicative of eutrophic conditions, and most are considerably greater than the chlorophyll *a* criterion of 15 µg L^{-1} derived for Chesapeake Bay based on a variety of associated water quality criteria (Harding et al. 2014). Because phytoplankton consume nutrients as they increase in biomass, chlorophyll *a* was inversely related to concentrations of nitrate and phosphate on the two

cruises (Fig. 4, $p<0.01$). Chlorophyll a concentrations >20-30 µg L^{-1} were associated with lower

concentrations of nitrate and phosphate, although the lowest nutrient concentrations, especially for

nitrate, were scattered over the entire range of chlorophyll a.

The chlorophyll a distributions on the salinity gradient exhibited higher values (>30 µg L^{-1}) at

salinities of 20-30 in the lower Delaware Bay (Fig. 5A, B, middle panels). At salinities <~20, chlorophyll a

value were 2-30 µg L^{-1}, whereas at salinities >20, there was a full range of chlorophyll a, with the highest

value > 100 µg L^{-1} in this salinity range. The highest chlorophyll a values consistently occurred on the

shoal flanks of the estuary at stations 10-03 to 10-05 NW of Cape May NJ and also at 25-06 to 25-07 on

the Delaware shoals near Bowers Beach. These are shallower estuarine flank areas which probably

have longer retention times and shallower mixing depths that allow greater phytoplankton

accumulation and drawdown of nutrient concentrations (Figs. 4, 5).

Dissolved Oxygen

There was little variation in dissolved oxygen (DO) across the salinity gradient (Fig. 5A, B, bottom

panels). In May, DO varied from 8-12 mg O_2 L^{-1}, which corresponds to about 20% below air saturation at

salinities <10 to about 20-30% above air saturation at salinities of 10-30. Similarly, in July, DO varied

from 6-9 mg O_2 L^{-1}, which corresponds to about 20% below saturation at salinities below 15 to about

20% above air saturation at salinities of 20-30. The patterns of DO along the salinity gradient were

similar in both months of sampling, with ~20% under-saturated conditions at lower salinities and 20%

over-saturated DO at higher salinities. No hypoxia in bottom waters was present in this dataset, and in

May there was no significant difference between paired surface and bottom samples ($p>0.10$). However,

in July the bottom samples were, on average, 0.9 mg O_2 L^{-1} lower than their surface counterparts

($p<0.01$). The pattern of oxygen concentrations in surface waters shown in Figs. 5A and B with

undersaturation at lower salinities and supersaturation at higher salinities suggests net ecosystem

respiration at salinities <10-15 and net ecosystem production at salinities >10.

<u>Respiration</u>

Respiration (R) varied over similar ranges for both cruises, -0.1 to -2.3 g O_2 m^{-3} d^{-1} in May and -0.3 to -1.8 g O_2 m^{-3} d^{-1} in July (Tables 1, 2). A Wilcoxon signed-rank test indicated that there was no significant difference in R between the two time periods (p>0.10). In May there was also no significant difference between respiration in surface and bottom waters (p>0.10), but respiration in July surface waters averaged -0.3 mg O_2 L^{-1} d^{-1} faster than in bottom waters (p<0.01).

Along the salinity gradient, respiration was distributed in a manner similar to chlorophyll *a*. Maximum values were found at salinities of 20-30 in the same shoal areas in which chlorophyll *a* reached its highest values (Fig. 5A, B, upper panels). As a result, respiration was strongly correlated with chlorophyll *a* in both time periods with highly significant r^2 values of 0.77-0.90 (Fig. 6), confirming that most of the respiration in the water column was related to phytoplankton, either as direct respiration by the phytoplankton itself or by associated heterotrophs. The overlap of surface and bottom water respiration in May can be seen in the top panel of Fig. 6, and the segregation of bottom water respiration to lower rates in July is clear in the lower panel of Fig. 6.

Because respiration was so strongly related to chlorophyll *a*, we normalized each value of respiration to the observed chlorophyll *a* at each station (Tables 1, 2). This resulted in a community respiration value per unit chlorophyll *a* of phytoplankton (R^B, g O_2 mg chla^{-1} h^{-1}). In May this reduced the range of R from >1 order of magnitude (ave = -0.68 ± 0.12 g O_2 m^{-3} d^{-1}) to a range of 2.5 for R^B (ave = -0.029 ± 0.004 g O_2 mg chla^{-1} h^{-1}). However, in July the range of R spanned a factor of 6 (ave = -0.83 ± 0.08 g O_2 m^{-3} d^{-1}), whereas R^B ranged over a factor of 8 in July (ave = -0.074 ± 0.009 g O_2 mg chla^{-1} h^{-1}).

Primary Production

There was a strong light dependence of C fixation (P_z, primary production) in both datasets (Fig. 2). The hyperbolic tangent provided easy parameter estimation for α (g C m^{-3} (E m^{-2})$^{-1}$), the light-dependent increase in C fixation with increasing PAR, and for P_m (g C m^{-3} d^{-1}), the light-independent, maximum rate of C fixation (Tables 3A and B, Fig. 2A lower panel). The exceptions were seven stations in the RM25 and RM40 transect lines in May. At these stations, which exhibited essentially linear relationships between C fixation and PAR (Sharp type 1 P-I curves, Fig. 2A upper panel), we obtained good estimates of α, but it was not possible to estimate P_m because P_z increased up to the highest PAR available (20 E m^{-2} d^{-1}, or about 45% of the maximum possible PAR on that day of the year, Fisher et al. 2003).

The photosynthetic parameters α and P_m (Tables 3A and B) varied over 1-2 orders of magnitude. In May α ranged over 0.05-0.94 g C m^{-3} (E m^{-2})$^{-1}$, with an average ± se = 0.24 ± 0.07 (Table 3A). In contrast, in July the range was larger at 0.05 – 1.42 (ave ± se = 0.38 ± 0.01, Table 3B). A Wilcoxon signed-rank test indicated that the July values of α were significantly greater than the May values at paired stations ($p<0.05$). P_m ranged over 0.6-4.9 g C m^{-3} d^{-1} in May, with an average of 2.4 ± 0.5 (Table 3A); in July the P_m values were similar (range = 0.7-4.5, ave ± se = 2.4 ± 0.3, Table 3B). A paired t test indicated no significant differences between the two sets of values of P_m at paired stations during May and July.

Both α and P_m were influenced by chlorophyll *a* concentrations (Figs. 7-8). There was a significant linear correlation between α and chlorophyll *a* in both the May and July datasets (Figs. 7A, B, upper panels). There was also a significant hyperbolic relationship between P_m and chlorophyll *a* in the July dataset (Fig. 7B, lower panel), but not for the May dataset (Fig. 7A, lower panel). Because of the relationships between α, P_m and chlorophyll a in Fig. 7, α and P_m were also significantly correlated in an hyperbolic relationship ($r^2 = 0.57$, $p<0.01$, Fig. 8). This relationship is similar to the one between P_m and chlorophyll *a* shown in the lower panel of Fig. 7B due to the strong linear relationship between α and

chlorophyll *a* shown in the upper panels of Fig. 7A and B.

As we did for the respiration data, we have removed the effect of phytoplankton biomass (chlorophyll *a*) on the photosynthetic parameters. We normalized α and P_m with the observed chlorophyll *a* to create the biomass-specific, light-dependent, photosynthetic parameter α^b with units of g C (E m^{-2})$^{-1}$ (mg chla)$^{-1}$ and the biomass-specific, light-independent, photosynthetic parameter P_m^b with units of g C (mg chla)$^{-1}$ d^{-1} (Tables 3A, B). These are useful for comparison with measurements of primary production in other Delaware Bay datasets and in other environments.

There was also an effect of the light extinction coefficient k (m^{-1}) on the photosynthetic parameters α, α^b, P_m, and P_m^b. In Fig. 9A, we have plotted both α and α^b as a function of k for both time periods. There were no significant relationships between α and k, but groups of data clump together largely related to the effects of varying chlorophyll *a* shown in Fig. 7. The lines in the upper panel of the figure are not regression lines, but appear to be related to ranges of chlorophyll *a*. When we removed the effect of chlorophyll *a* by plotting α^b versus k, a weak exponential relationship emerged that was statistically significant ($r^2 = 0.25$, p<0.05, Fig. 9A, lower panel). We found somewhat similar relationships between P_m and k (Fig. 9B); however, in this case, the classes of ranges of chlorophyll *a* were less distinct than those of α (upper panel, Fig. 9B), and there was no significant effect of k on P_m^b (lower panel, Fig. 9B).

Primary productivity (P, g C m^{-2} d^{-1}) ranged over about an order of magnitude (0.5-6 g C m^{-2} d^{-1}), and was significantly higher in July than in May (Tables 3A, B). The highest values of P occurred at stations RM 10-04, 10-05, 25-06, and 25-07 in May, and at RM 10-04, 10-05, 25-07, and 25-10 in July (upper panel, Fig. 10). Because P was computed using α and P_m, P is also related to chlorophyll *a* and k (Fig. 10), as were α and P_m (Fig. 9). In the upper panel of Fig. 10 we show an apparently linear relationship between P and chlorophyll *a* in May, but an hyperbolic relationship in July, probably due to warmer temperatures. In contrast, in the lower panel of Fig. 10 we show a single inverse exponential

relationship between P and k for both months combined. The tendency for lower P in May and higher P

in July is clear in this figure, but the data are fit by a single exponential relationship which is highly

significant ($p<0.01$). The relationships in Figs. 6-10 potentially provide an empirical basis for estimating

the photosynthetic parameters α, P_m, and P using relatively simple field measurements of chlorophyll *a*,

k, and PAR.

Conclusions and Synthesis

It is clear that Delaware Bay is nutrient-enriched from its upstream basin. Nitrate, in particular, is quite high in the freshwater end-member (100-120 µM), essentially equivalent to concentrations in the Susquehanna River that largely drive eutrophication and hypoxia in the mainstem of Chesapeake Bay (Fisher et al. 1988, Glibert et al. 1995, Kemp et al. 2005). Nutrient concentrations within the Delaware estuary are typically above levels considered saturating for phytoplankton growth, and chlorophyll a concentrations are frequently quite high (>50 µg L^{-1}), values associated with poor water quality and hypoxia in Chesapeake Bay (Harding et al. 2014). There are also significant correlations between chlorophyll a, nutrients, respiration, and primary production, indicating clear linkages between the water column parameters measured in this study. Rates of both respiration and primary productivity are high. Why then do we observe so little hypoxia in Delaware Bay?

There is some hypoxia, of course, in the upper Delaware estuary. Both surface and bottom waters with salinities <10-15 were ~20% undersaturated in O_2 compared to atmospheric equilibrium, and most of the stations down-estuary with salinities >10-15 were ~20% supersaturated. This indicates regions of net respiration and consumption of organic matter in lower salinity areas as well as a region of net primary production of organic matter at higher salinities. However, compared to the near anoxia of the Chesapeake Bay mainstem and some tributaries in summer (e.g., Hagy et al. 2004), the impact of the nutrients on Delaware Bay is relatively small in terms of dissolved oxygen.

The difference between these two estuarine systems lies in their physics. Chesapeake Bay was overdeepened during the last glacial maximum and is still filling in the former Susquehanna River valley that we now call Chesapeake Bay. Delaware Bay has access to larger sand supplies which has filled in the former Delaware River valley now known as the lower Delaware estuary. Furthermore, the lower Delaware estuary is shallow and funnel-shaped, amplifying the tidal amplitudes towards the freshwater end. This results in enhanced flushing and mixing energy compared to Chesapeake Bay, which widens

16

from its mouth, resulting in damped tides, less flushing, and low mixing energy in its mid-section. As a result, Chesapeake Bay is density-stratified by for much of the year, cutting off the supply of atmospheric O_2 from bottom waters and enhancing hypoxia. In contrast, shallow Delaware Bay is mixed by big tides and is frequently unstratified by density, allowing ventilation of biologically driven oxygen deficits and surpluses in low and high salinity waters, respectively, in both surface and bottom waters, despite the development of relatively high values of phytoplankton biomass. The contrast between these two adjacent estuarine systems is quite striking.

Is the water quality in Delaware Bay cause for concern? In the two time periods examined here (May and July 2014), there was little deviation from O_2 atmospheric equilibrium in surface or bottom waters, indicating minimal impact on dissolved O_2. Much of the nutrients appear to be assimilated in the lower bay where the subsequent organic matter is subject to dispersal on the continental shelf. However, chlorophyll a concentrations were quite high (>100 μg L^{-1}) in May, and values of that magnitude are often associated with harmful algal blooms, which can have significant impacts on fisheries, recreational activities, and human health. Reducing nutrient inputs in the upper estuary and in the river basin would reduce the potential for harmful algal blooms in the lower bay.

References

Bevington, P. R. 1969. Data Reduction and Error Analysis for the Physical Sciences. McGraw-Hill Book Co., NY, 336 pps.

Colt, J. 1984. Computation of dissolved gas concentrations in water as functions of temperature, salinity, and pressure. Amer. Fish. Soc. Spec. Pub. 14

Fisher, T. R., L. W. Harding, D. W. Stanley, and L. G. Ward. 1988. Phytoplankton, nutrients, and turbidity in the Chesapeake, Delaware, and Hudson River estuaries. Est. Coastal Shelf Sci. 27: 61-93

Fisher, T. R., J. M. Melack, J. Grobbellar, and R. W. Howarth. 1995. Nutrient limitation of phytoplankton and eutrophication of estuarine and marine waters. pps. 301-322 IN: H. Tiessen (ed.) Phosphorus cycling in Terrestrial and Aquatic Ecosystems. SCOPE, Wiley.

Fisher, T. R., A. B. Gustafson, K. Sellner, R. Lacuture, L. W. Haas, R. Magnien, R. Karrh, and B. Michael. 1999. Spatial and temporal variation in resource limitation in Chesapeake Bay. Mar. Biol. 133: 763-778

Fisher, T. R., A. B. Gustafson, G. R. Radcliffe, K. L. Sundberg, and J. C. Stevenson. 2003. A long-term record of photosynthetically active radiation (PAR) and total solar energy at 38.6° N, 78.2° W. Estuaries 26: 1450-1460

Glibert, P. M., D. J. Conley, T. R. Fisher, L. W. Harding, Jr., and T. C. Malone. 1995. Dynamics of the 1990 winter/spring bloom in Chesapeake Bay. Mar. Ecol. Prog. Ser. 122:27-43

Hagy, J. D., W. R. Boynton, C. W. Keefe, and K. V. Wood. 2004. Hypoxia in Chesapeake Bay, 1950-2001: long-term change in relation to nutrient loading and river flow. Estuaries 27: 634-658

Harding, Jr., L. W., R. A. Batiuk, T. R. Fisher, C. L. Gallegos, T. C. Malone, W. D. Miller, M. R. Mulholland, H. W. Paerl, and P. Tango. 2014. Scientific bases for numerical chlorophyll criteria in Chesapeake Bay. Estuaries and Coasts 37: 134-148

Jassby, A. D. and T. Platt 1976. Mathematical formulation of the relationship between photosynthesis and light for phytoplankton. Limnol. Oceanogr. 21: 540-547

Kana, T. M., C. Darkangelo, M. D. Hunt, J. B. Oldham, G. E. Bennett, and J. C. Cornwell. 1994. Membrane inlet mass spectrometer for rapid high-precision determination of N_2, O_2, and Ar in environmental water samples. Anal. Chem. 66:4166-4170

Kemp, W. M., W. R. Boynton, J. E. Adolf, D. F. Boesch, W. C. Boicourt, G. Brush, J. C. Cornwell, T. R. Fisher, P. M. Glibert, J. D. Hagy, L. W. Harding, E. D. Houde, D. G. Kimmel, W. D. Miller, R. I. E. Newell, M.

R. Roman, E. M. Smith, J. C. Stevenson. 2005. Eutrophication of Chesapeake Bay: Historical trends and ecological interactions. Mar. Ecol. Prog. Ser. 303: 1-29

Lane, L., S. Rhoades, C. Thomas, and L. Van Heukelem. 2000. Standard Operating Procedures of the Analytical Services Laboratory of the Horn Point Laboratory, Center for Environmental Science, University of Maryland. Tech. Rep. No. TS-264-00

Sharp, J. H., K. Yoshiyama, A. E. Parker, M. C. Schwartz, S. E. Curless, A. Y. Beauregard, J. E. Ossolinkski, and A. R. Davis. 2009. A biogeochemical view of estuarine Eutrophication: seasonal and spatial trends and correlations in the Delaware Estuary. Estuaries and Coasts 32: 1023-1043

Sharp, J. H. 2013. Biogeochemical Methods Manual. School of Marine Science and Policy, College of Earth, Ocean, and Environment, University of Delaware.

Table 1. Data Summary for Delaware Bay (19 May 2014). Abbreviations: Temp = temperature, ext. coef. = extinction coefficient, NH_4 = ammonium, NO_3 = nitrate + nitrite, PO_4 = soluble reactive phosphate, Chla = chlorophyll a , R = Respiration, and R^B = respiration normalized per unit Chla.

Station	Salinity	Temp °C	mg O_2 L^{-1} DO	ext. coef. k, m^{-1}	NH_4	µM NO_3	PO_4	Chla, mg m^{-3} ave	se	g O_2 m^{-3} d^{-1} R	se	g O_2 (mg Chla)$^{-1}$ d^{-1} R^B	se
RM10-01 top	25.3	16.0	9.68	3.13	1.88	0.5	0.14	41.2	1.1	-1.30	0.04	-0.032	0.026
RM10-02 top	22.8	15.8	9.04	3.01	0.94	11.0	0.13	26.8	0.4	-0.63	0.04	-0.024	0.014
RM10-03 top	22.2	16.9	9.97	1.93	0.89	2.4	0.11	49.8	1.2	-1.11	0.01	-0.022	0.023
RM10-04 top	22.4	17.5	9.07	2.80	0.46	0.2	0.11	62.6	7.5	-1.90	0.08	-0.030	0.120
RM10-05 top	19.5	18.3	9.86	4.29	0.43	0.0	0.12	108.3	7.0	-2.29	0.06	-0.021	0.065
RM25-06 top	20.6	18.4	10.05	3.47	0.32	0.0	0.11	56.5	10.6	-1.24	0.12	-0.022	0.188
RM25-07 top	20.0	17.5	8.96	2.77	0.96	1.0	0.11	57.0	11.0	-0.31	0.08	-0.005	0.192
RM25-08 top	12.9	17.7	8.83	1.98	2.35	46.5	0.33	17.7	0.0	-0.61	0.02	-0.034	0.003
RM25-09 top	14.8	17.2	8.83	2.14	1.84	40.6	0.17	16.5	0.2	-0.52	0.01	-0.031	0.012
RM25-10 top	13.8	18.0	11.63	2.61	0.56	42.2	0.07	25.6	1.3	-0.60	0.04	-0.023	0.049
RM40-11 top	5.7	18.6	8.04	5.25	4.10	73.5	1.26	4.2	0.4	-0.30	0.01	-0.072	0.103
RM40-12 top	5.6	18.4	8.19	4.94	4.21	75.4	1.30	4.2	0.1	-0.22	0.04	-0.051	0.027
RM40-13 top	6.6	18.2	7.60	3.73	4.41	72.5	1.24	4.2	0.1	-0.25	0.02	-0.059	0.012
RM40-14 top	7.4	18.5	8.48	3.18	4.38	72.6	1.27	5.4	0.8	-0.22	0.04	-0.041	0.157
RM40-15 top	7.4	18.9	8.65	3.62	4.48	66.2	1.08	7.4	0.2	-0.40	0.02	-0.053	0.029
RM-55-ETM top	0.5	18.1	8.08	--	0.94	106.0	1.34	9.2	0.2	-0.40	0.02	-0.043	0.024
RM10-02 bottom	25.6	15.5	9.08	--	2.68	7.7	0.13	16.1	0.1	-0.63	0.03	-0.039	0.008
RM25-06 bottom	20.6	18.1	11.36	--	1.28	0.1	0.15	62.9	3.4	-1.35	0.03	-0.021	0.053
RM25-07 bottom	20.4	16.8	10.54	--	2.01	9.0	0.10	52.0	5.2	-0.82	0.02	-0.016	0.101
RM25-08 bottom	16.9	17.2	8.54	--	4.77	44.3	0.45	15.4	0.2	-0.35	0.04	-0.023	0.014
RM40-10 bottom	13.8	17.8	8.98	--	1.05	42.5	0.10	19.9	2.8	-0.12	0.01	-0.006	0.138
RM40-12 bottom	8.6	17.7	7.66	--	5.09	71.9	1.30	4.5	0.9	0.13	0.01	0.029	0.203
RM40-14 bottom	8.0	18.3	7.76	--	5.93	66.1	1.28	5.7	0.0	-0.15	0.02	-0.027	0.009
minimum =	0.5	15.5	7.60	1.93	0.32	0.0	0.07	4.2		-2.29		-0.072	
maximum =	25.6	18.9	11.63	5.25	5.93	106.0	1.34	108.3		0.13		0.029	
average =	14.8	17.6	9.08	3.26	2.43	37.0	0.54	29.3		-0.68		-0.029	
std. error =	1.5	0.2	0.23	0.26	0.38	7.0	0.11	5.7		0.12		0.004	

Table 2. Data Summary for Delaware Bay (21 July 2014). Abbreviations: Temp = temperature, NH_4 = ammonium, NO_3 = nitrate + nitrite, PO_4 = soluble reactive phosphate, Chla = chlorophyll a , R = Respiration, and R^B = respiration normalized per unit Chla.

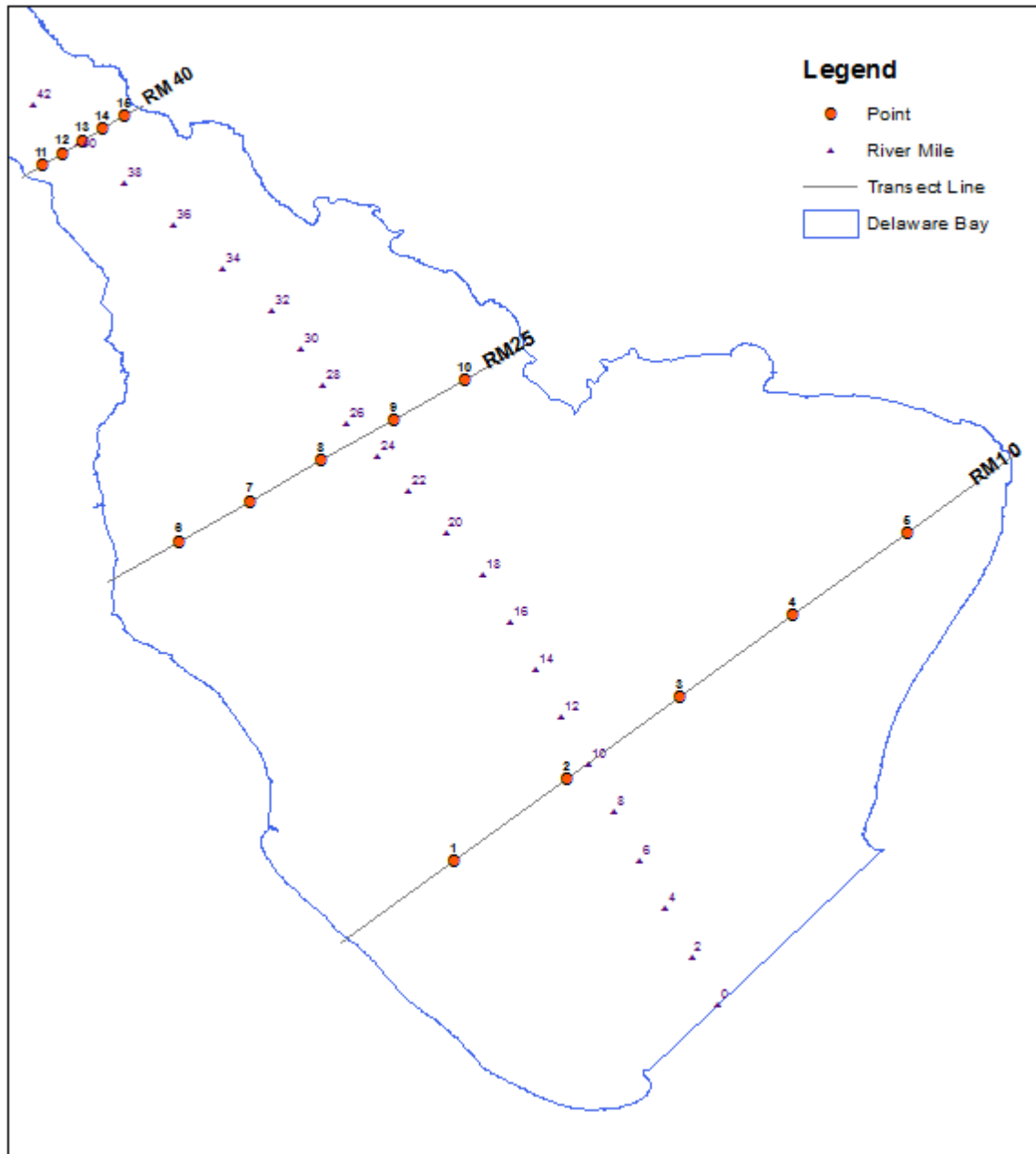| Station	Salinity	Temp	mg O_2 L^{-1} DO	ext. coef. k, m^{-1}	NH_4	μM NO_3	PO_4	Chla, mg m^{-3} ave	se	g O_2 m^{-3} d^{-1} respiration	se	g O_2 (mg Chla)$^{-1}$ d^{-1} R^B	se
RM10-01 top	27.3	22.2	6.34	1.27	8.18	2.2	0.58	10.2	0.1	-0.54	0.01	-0.052	0.012
RM10-02 top	28.4	21.0	7.89	1.21	0.61	0.1	0.18	13.5	0.4	-0.87	0.03	-0.064	0.033
RM10-03 top	24.9	23.3	7.99	1.49	0.49	0.1	0.13	16.3	0.2	-1.00	0.01	-0.061	0.010
RM10-04 top	22.9	23.9	8.24	1.52	0.37	0.1	0.09	37.1	0.6	-1.44	0.01	-0.039	0.016
RM10-05 top	19.1	24.6	8.45	2.54	1.47	12.1	0.09	61.0	5.3	-1.77	0.03	-0.029	0.088
RM25-06 top	21.7	26.0	8.10	1.81	1.08	4.8	0.38	59.2	0.2	-1.69	0.08	-0.028	0.004
RM25-07 top	20.2	25.6	9.07	1.48	0.34	6.2	0.10	53.6	2.6	-1.54	0.02	-0.029	0.048
RM25-08 top	15.6	25.7	7.91	1.15	0.37	38.7	1.12	20.1	0.3	-0.90	0.03	-0.045	0.016
RM25-09 top	18.2	25.1	6.81	1.17	0.43	32.4	1.15	16.1	0.4	-0.81	0.10	-0.050	0.026
RM25-10 top	17.3	25.3	7.82	1.16	2.82	34.9	1.38	13.4	0.2	-0.96	0.03	-0.072	0.018
RM40-11 top	8.0	26.6	6.77	4.62	0.37	78.5	2.16	8.8	0.0	-0.78	0.03	-0.089	0.006
RM40-12 top	7.7	27.1	6.92	2.15	0.21	83.0	2.03	5.3	0.0	-0.49	0.03	-0.093	0.005
RM40-13 top	7.9	27.1	6.87	1.86	0.25	80.2	2.11	6.8	0.2	-0.35	0.01	-0.051	0.035
RM40-14 top	11.5	26.4	6.52	4.90	0.32	69.5	2.01	7.4	0.2	-0.46	0.03	-0.063	0.022
RM40-15 top	11.3	26.2	7.07	8.20	0.29	64.7	2.09	7.4	1.0	-0.65	0.06	-0.087	0.131
RM-55-ETM top	2.4	26.8	6.32	--	0.45	114.0	2.03	9.1	0.1	-0.50	0.03	-0.055	0.012
RM10-02 bottom	30.0	19.5	6.96	--	3.03	0.3	0.72	2.3	0.0	-0.50	0.03	-0.219	0.022
RM10-03 bottom	24.5	23.1	6.92	--	6.36	0.2	0.42	8.6	0.4	-0.78	0.09	-0.090	0.052
RM25-06 bottom	21.6	25.3	6.63	--	7.60	6.2	0.95	18.6	0.1	-0.91	0.04	-0.049	0.006
RM25-07 bottom	21.5	24.8	9.15	--	4.84	9.0	0.65	22.1	0.6	-1.10	0.01	-0.050	0.029
RM25-08 bottom	19.5	24.6	6.75	--	3.27	25.9	1.37	7.8	0.1	-0.69	0.01	-0.088	0.010
RM40-10 bottom	17.7	25.0	6.30	--	7.17	33.7	1.69	4.1	0.0	-0.46	0.02	-0.113	0.012
RM40-12 bottom	13.1	25.6	6.15	--	0.21	75.1	2.16	3.2	0.0	-0.32	0.01	-0.102	0.008
RM40-13 bottom	13.7	25.6	6.21	--	<0.21	67.1	2.24	3.4	0.1	-0.50	0.05	-0.148	0.029
minimum =	2.4	19.5	6.15	1.15	0.21	0.1	0.09	2.3		-1.77		-0.219	
maximum =	30.0	27.1	9.15	8.20	8.18	114.0	2.24	61.0		-0.32		-0.028	
average =	17.7	24.8	7.26	2.44	2.20	34.9	1.18	17.3		-0.83		-0.074	
std. error =	1.5	0.4	0.18	0.51	0.57	7.2	0.16	3.6		0.08		0.009	

Table 3A. Primary Production Parameters: 19 May 2014. Abbreviations: r^2 = coefficient of determination, p = probability due to chance, α = initial slope of light-dependent primary production, $α^b$ = α normalized to chlorophyll a, P_m = maximum rate of primary production, P_m^b = Pm normalized to chlorophyll a, k = light extinction coefficient in the water column, and P = primary productivity (integrated rate of C fixation in the water column).

Sample	r^2	regression p	$gC\ m^{-3}\ (E\ m^{-2})^{-1}$ α	p(α)	$gC\ (E\ m^{-2})^{-1}\ (mg\ chla)^{-1}$ $α^b$	$gC\ m^{-3}\ d^{-1}$ P_m	$p(P_m)$	$gC\ (mg\ chla)^{-1}\ d^{-1}$ P_m^b	ext. coef. k, m^{-1}	$gC\ m^{-2}\ d^{-1}$ P
RM10-01	0.99	<0.01	0.122 ± 0.010	<0.01	0.0030	1.60 ± 0.09	<0.01	0.0388	3.13	0.82
RM10-02	0.99	<0.01	0.0812 ± 0.0067	<0.01	0.0030	0.664 ± 0.032	<0.01	0.0248	3.01	0.44
RM10-03	0.98	<0.01	0.102 ± 0.015	<0.01	0.0200	0.918 ± 0.086	<0.01	0.0184	1.93	1.04
RM10-04	0.91	<0.05	0.234 ± 0.049	<0.05	0.0037	2.09 ± 0.27	<0.01	0.0334	2.80	1.68
RM10-05	0.92	<0.01	0.691 ± 0.117	<0.01	0.0064	3.38 ± 0.25	<0.01	0.0313	4.29	2.17
RM25-06	0.96	<0.01	0.512 ± 0.072	<0.01	0.0091	3.62 ± 0.26	<0.01	0.0641	3.47	2.48
RM25-07	0.97	<0.01	0.394 ± 0.052	<0.01	0.0069	4.93 ± 0.55	<0.01	0.0865	2.77	3.29
RM25-08	0.99	<0.01	0.230 ± 0.013	<0.01	0.0130	3.45 ± 0.16	<0.01	0.1949	1.98	2.47
RM25-09	0.96	<0.01	0.0920 ± 0.0092	<0.05	0.0056	indeterminate		--	2.14	1.41
RM25-10	0.95	<0.01	0.119 ± 0.020	<0.05	0.0046	indeterminate		--	2.61	1.45
RM40-11	0.99	<0.01	0.0862 ± 0.0034	<0.01	0.0205	indeterminate		--	5.25	0.53
RM40-12	0.98	<0.01	0.0562 ± 0.0071	<0.01	0.0134	indeterminate		--	4.94	0.35
RM40-13	0.95	<0.01	0.0682 ± 0.0118	<0.05	0.0161	indeterminate		--	3.73	0.60
RM40-14	0.99	<0.01	0.0968 ± 0.0024	<0.01	0.0179	indeterminate		--	3.18	0.87
RM40-15	0.95	<0.01	0.0934 ± 0.0088	<0.05	0.0126	indeterminate		--	3.62	0.72
RM55-ETM	0.99	<0.01	0.0529 ± 0.0021	<0.01	0.0058	0.648 ± 0.017	<0.01	0.0707	--	--
minimum =			0.053		0.0030	0.65			1.93	0.35
maximum =			0.691		0.0205	4.93			5.25	3.29
average =			0.189		0.0101	2.37			3.26	1.35
std. error =			0.047		0.0015	0.51			0.26	0.23

Table 3B. Primary Production Parameters: 21 July 2014. Abbreviations: r^2 = coefficient of determination, p = probability due to chance, α = initial slope of light-dependent primary production, α^b = α normalized to chlorophyll a, P_m = maximum rate of primary production, P_m^b = Pm normalized to chlorophyll a, k = light extinction coefficient in the water column, and P = primary productivity (integrated rate of C fixation in the water column).

| Sample	r^2	regression p	$gC\ m^{-3}\ (E\ m^{-2})^{-1}$ α	$p(\alpha)$	$gC\ (E\ m^{-2})^{-1}\ (mg\ chl\,a)^{-1}$ α^b	$gC\ m^{-3}\ d^{-1}$ P_m	$p(P_m)$	$gC\ (mg\ chl\,a)^{-1}\ d^{-1}$ P_m^b	ext. coef. k, m^{-1}	$gC\ m^{-2}\ d^{-1}$ Prim. Prod.
RM10-01	0.81	<0.05	0.410 ± 0.121	<0.05	0.0401	1.79 ± 0.23	<0.01	0.1750	1.27	3.950
RM10-02	0.97	<0.05	0.346 ± 0.040	<0.05	0.0255	1.38 ± 0.09	<0.01	0.1019	1.21	3.320
RM10-03	0.99	<0.01	0.605 ± 0.045	<0.01	0.0370	2.46 ± 0.10	<0.01	0.1506	1.49	4.551
RM10-04	0.71	=0.07	0.571 ± 0.184	=0.05	0.0154	3.26 ± 0.50	<0.01	0.0880	1.52	5.768
RM10-05	0.98	<0.01	1.42 ± 0.10	<0.01	0.0233	4.51 ± 0.12	<0.01	0.0740	2.54	5.391
RM25-06	0.88	<0.05	0.399 ± 0.090	<0.05	0.0067	2.94 ± 0.36	<0.01	0.0496	1.81	3.941
RM25-07	0.98	<0.05	1.09 ± 0.12	<0.05	0.0203	3.17 ± 0.13	<0.01	0.0591	1.48	6.109
RM25-08	0.99	<0.01	0.219 ± 0.020	<0.01	0.0109	3.03 ± 0.28	<0.01	0.1505	1.15	4.456
RM25-09	0.96	<0.01	0.182 ± 0.029	<0.01	0.0113	3.59 ± 1.00	<0.05	0.2232	1.17	4.310
RM25-10	0.97	<0.01	0.371 ± 0.047	<0.01	0.0276	2.96 ± 0.21	<0.01	0.2206	1.16	5.834
RM40-11	0.99	<0.01	0.0552 ± 0.0032	<0.01	0.0063	1.26 ± 0.16	<0.01	0.1437	4.62	0.333
RM40-12	0.95	<0.01	0.0469 ± 0.0082	<0.05	0.0089	1.08 ± 0.43	=0.08	0.2053	2.15	0.638
RM40-13	0.99	<0.01	0.0645 ± 0.0049	<0.01	0.0095	0.690 ± 0.038	<0.01	0.1016	1.86	0.728
RM40-14	0.99	<0.01	0.111 ± 0.006	<0.01	0.0151	1.59 ± 0.09	<0.01	0.2160	4.90	0.546
RM40-15	0.99	<0.01	0.115 ± 0.008	<0.01	0.0155	1.80 ± 0.15	<0.01	0.2419	8.20	0.347
RM55-ETM	0.98	<0.01	0.144 ± 0.020	<0.01	0.0159	3.34 ± 1.03	<0.05	0.3689	--	--
minimum =			0.047		0.0063	0.69		0.050	1.15	0.333
maximum =			1.420		0.0401	4.51		0.369	8.20	6.109
average =			0.384		0.0181	2.43		0.161	2.44	3.348
std. error =			0.097		0.0026	0.27		0.021	0.51	0.570

Figure 1. Map of sampling locations in Delaware Bay at River Mile (RM) 40, 25, and 10.
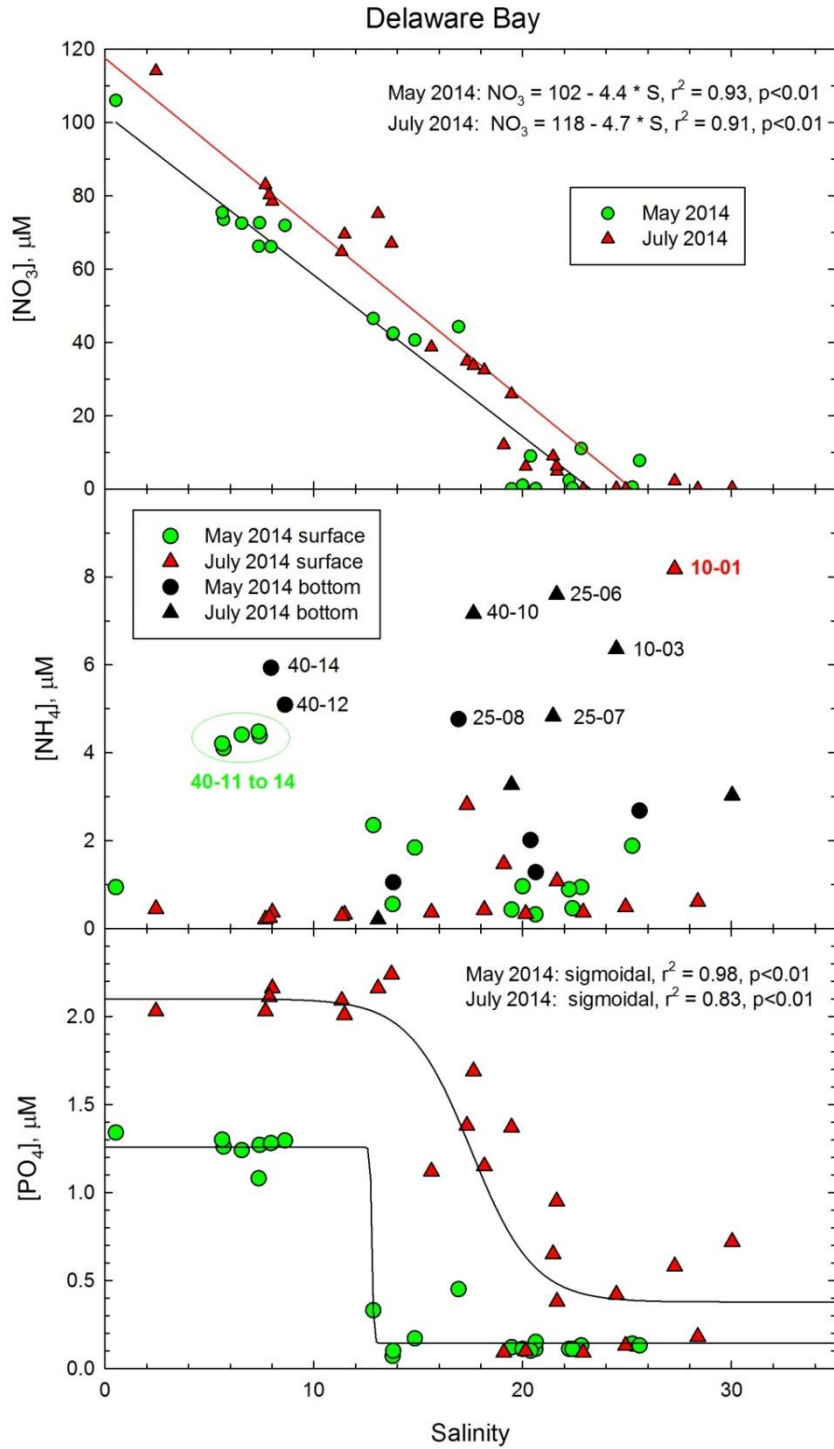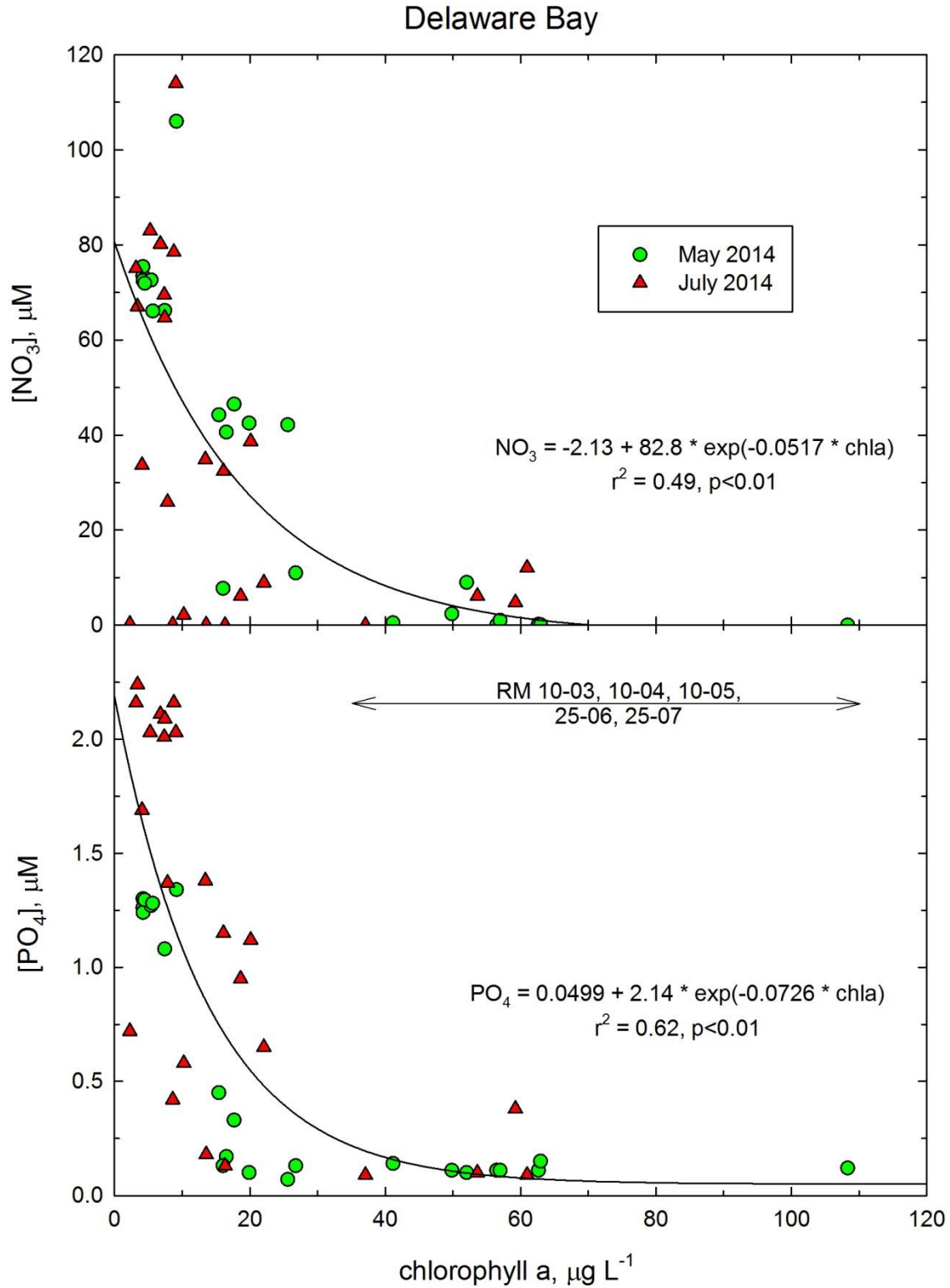
May 2014
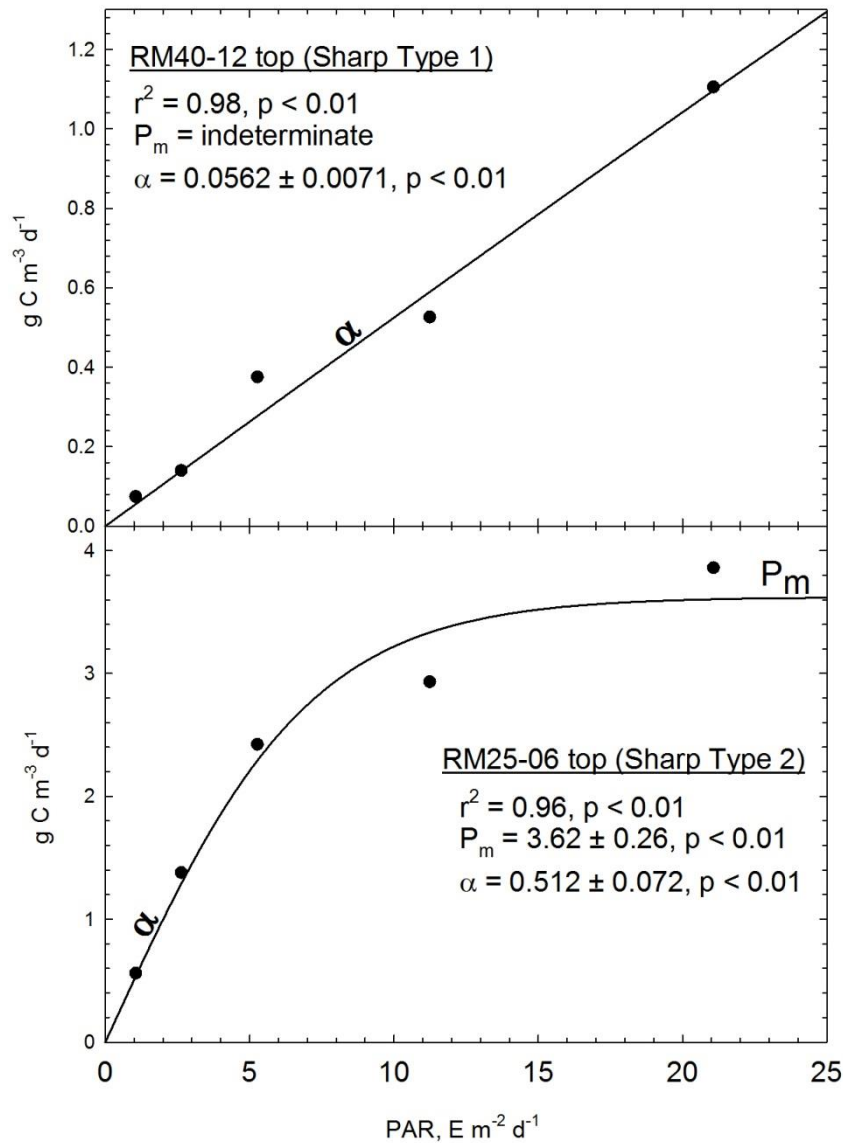
Figure 2A. Two examples of the hyperbolic tangent fit of eq. 7 to production vs PAR data. The top panel is essentially a linear response to PAR (Sharp type 1). The initial linear response to PAR, α, was estimated, but P_m, the maximum rate of primary production, could not be determined in this example. The bottom panel is an example where primary production was essentially saturated by PAR at PAR > 20 E m^{-2} d^{-1} (Sharp type 2), and both α and P_m were estimated. There were no examples of Sharp type 3 (light inhibition) in this dataset.
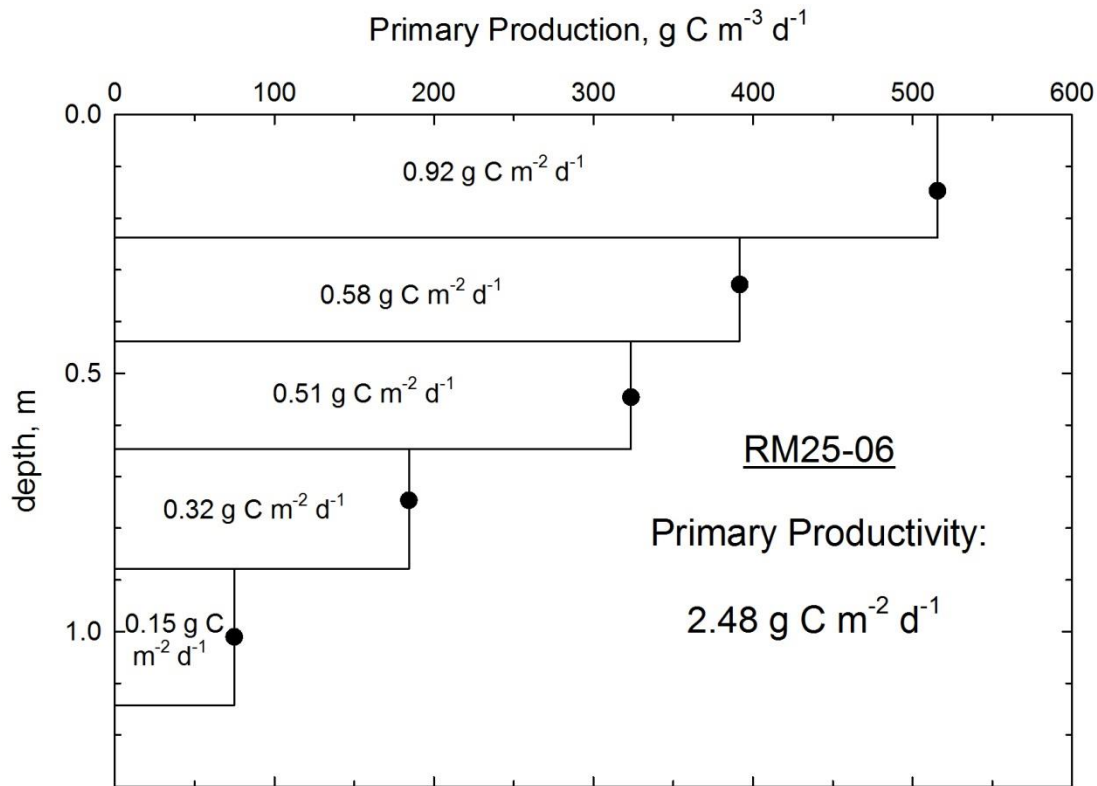
Figure 2B. Example of depth integration to obtain integrated primary productivity (P, g C m^{-2} d^{-1}) at each station from the individual measurements of primary production (P$_Z$, g C m^{-3} d^{-1}) at fixed light depths of 3-60% ambient light. Light depths (I$_Z$/I$_0$) were converted to water column depths using the measured extinction coefficient (k, m^{-1}) at each station (eq. 8), and primary productivity in each depth interval (ΔZ) was computed as P$_Z$ * ΔZ and summed vertically for the total station primary productivity (eq. 9).

Figure 3. Mixing curves for major nutrients in Delaware Bay on the two sampling dates.

Figure 4. Inverse relationships of chlorophyll *a* with nitrate and phosphate concentrations in the two time periods.

Delaware Bay (May 2014)
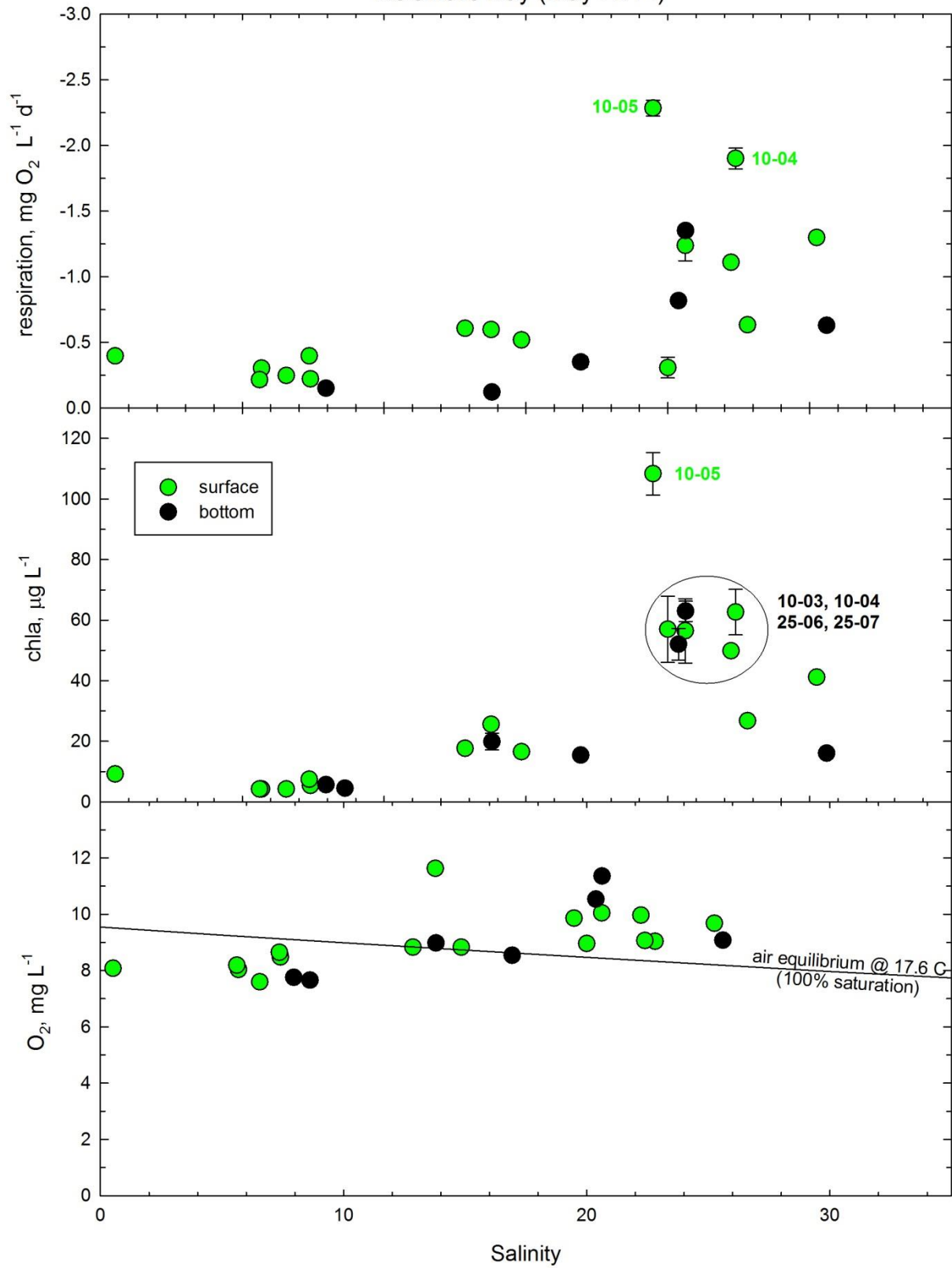
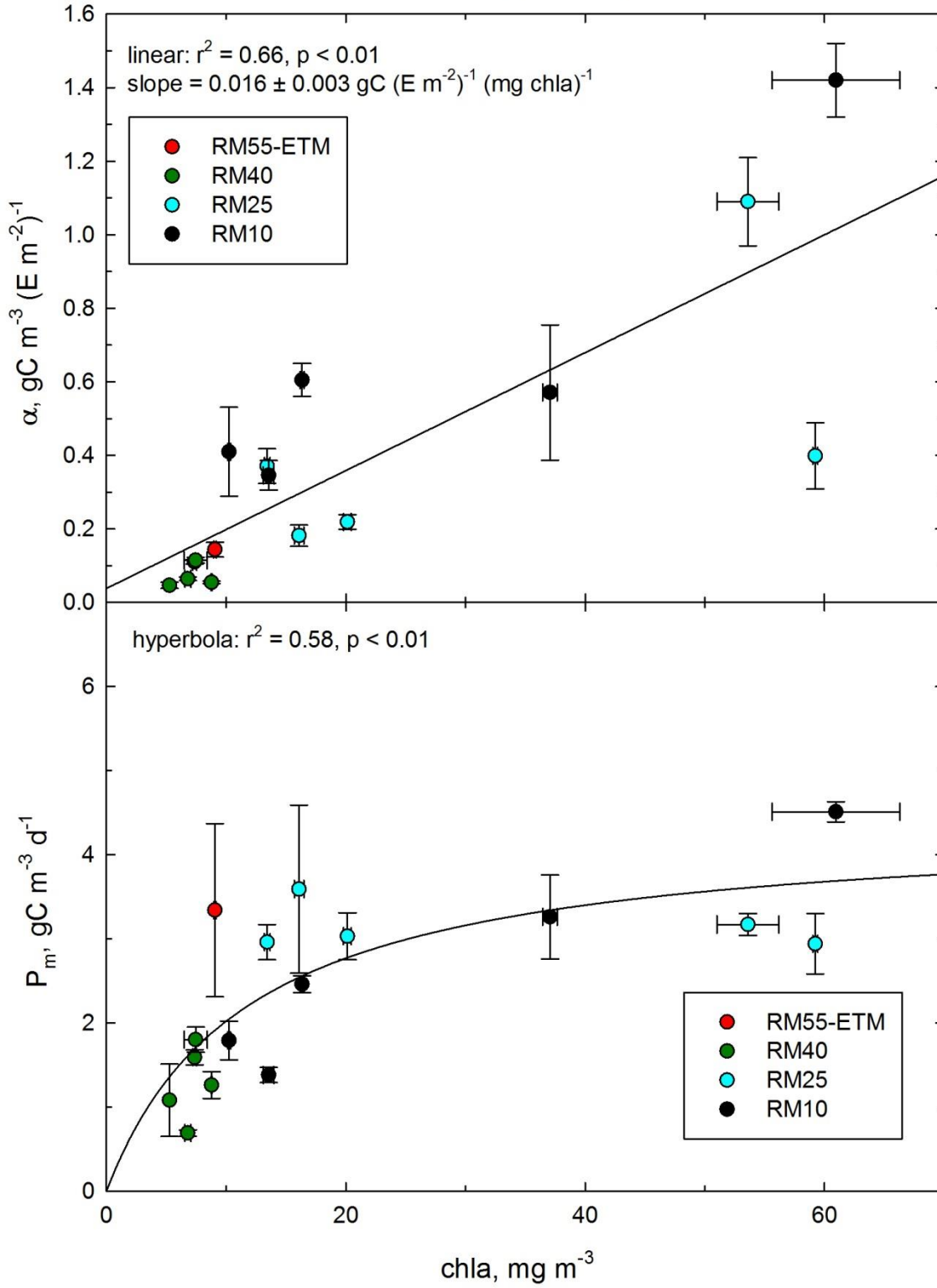**Figure 5A**. Respiration, chlorophyll a, and dissolved oxygen in Delaware Bay for May 2014. Air equilibrium for O_2 was calculated from temperature and salinity using Colt (1984).

Delaware Bay (July 2014)
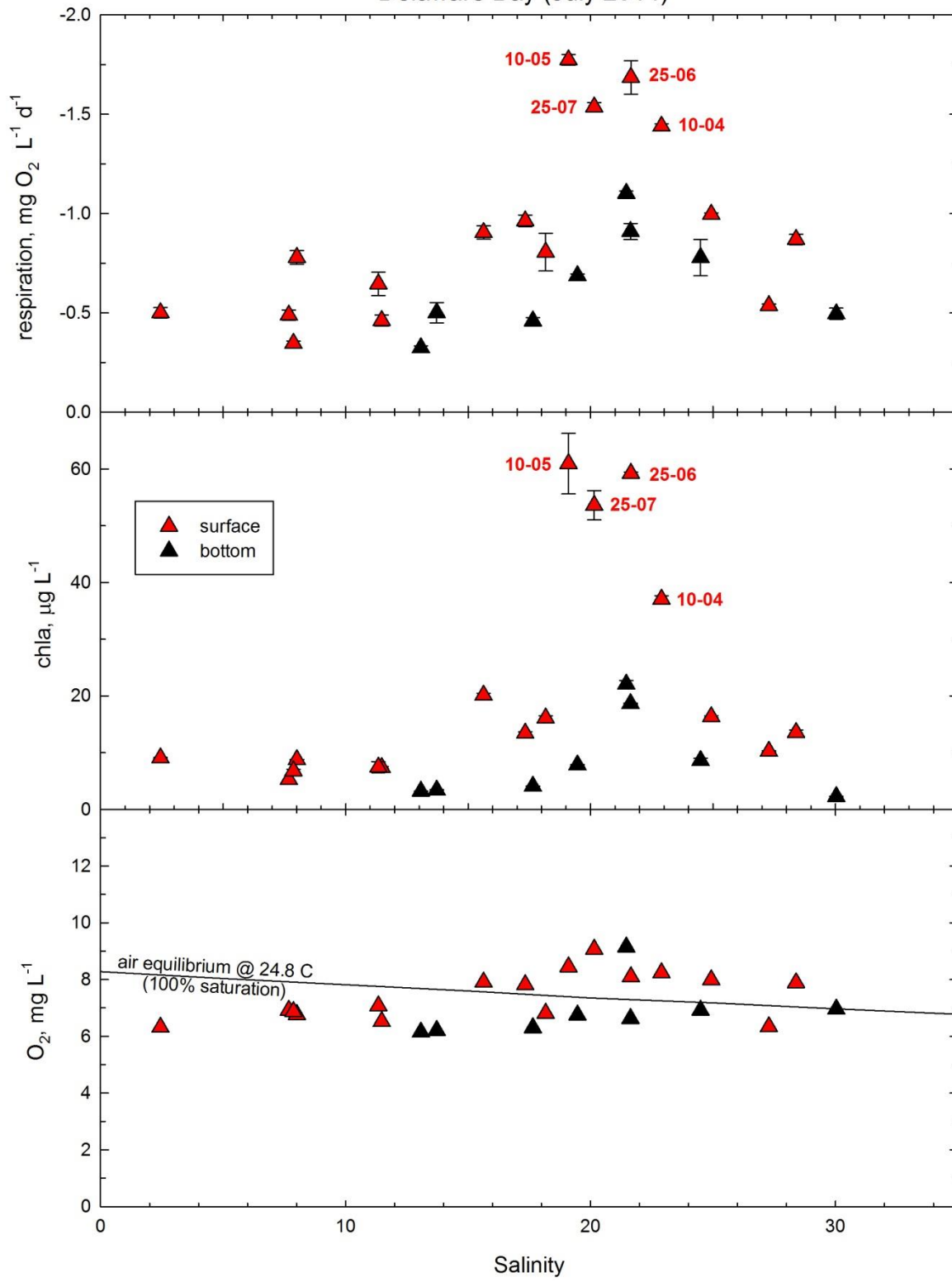
Figure 5B. Respiration, chlorophyll a, and dissolved oxygen in Delaware Bay for July 2014. Air equilibrium for O_2 was calculated as in Fig. 5A.
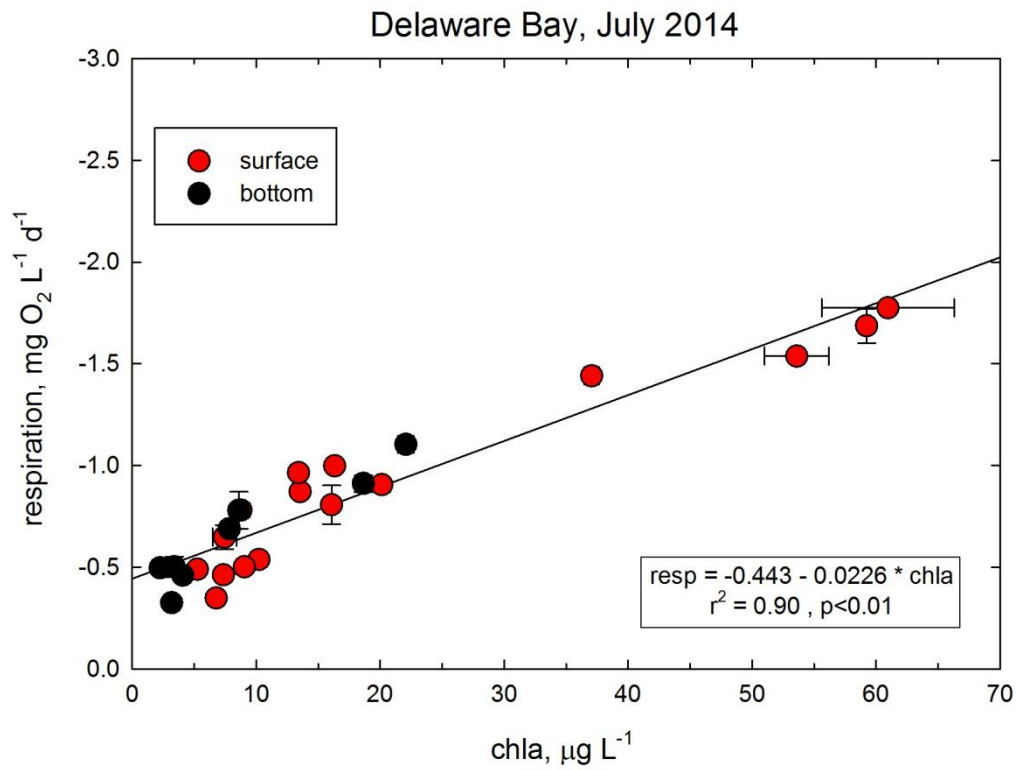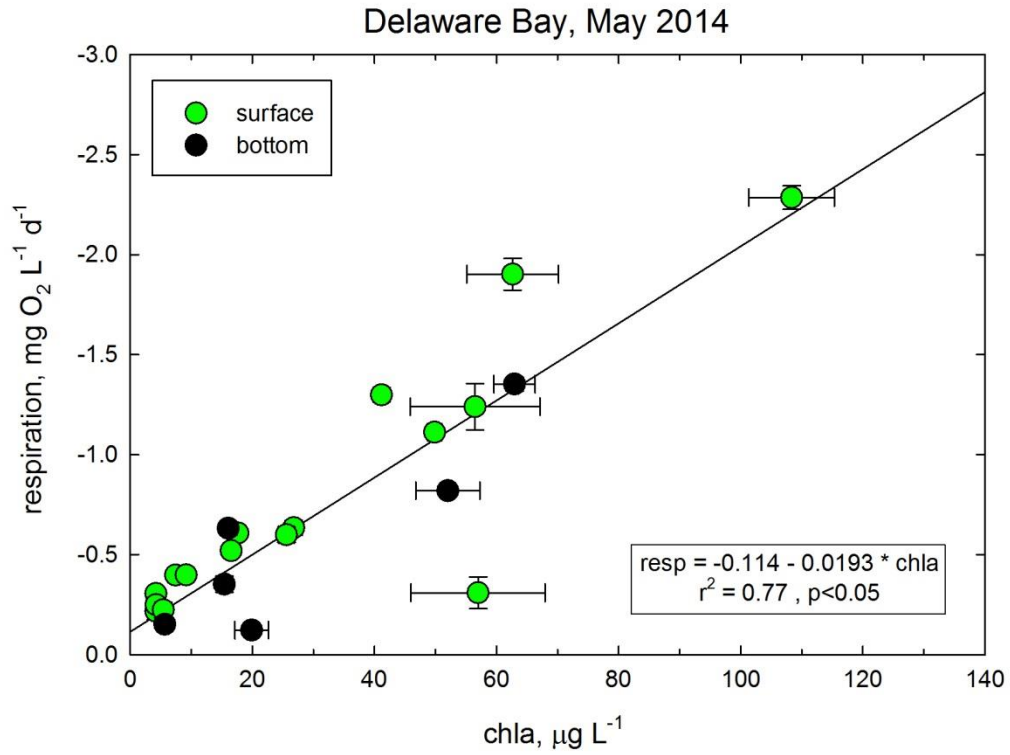
Figure 6. Effect of chlorophyll *a* on respiration in Delaware Bay for both time periods.
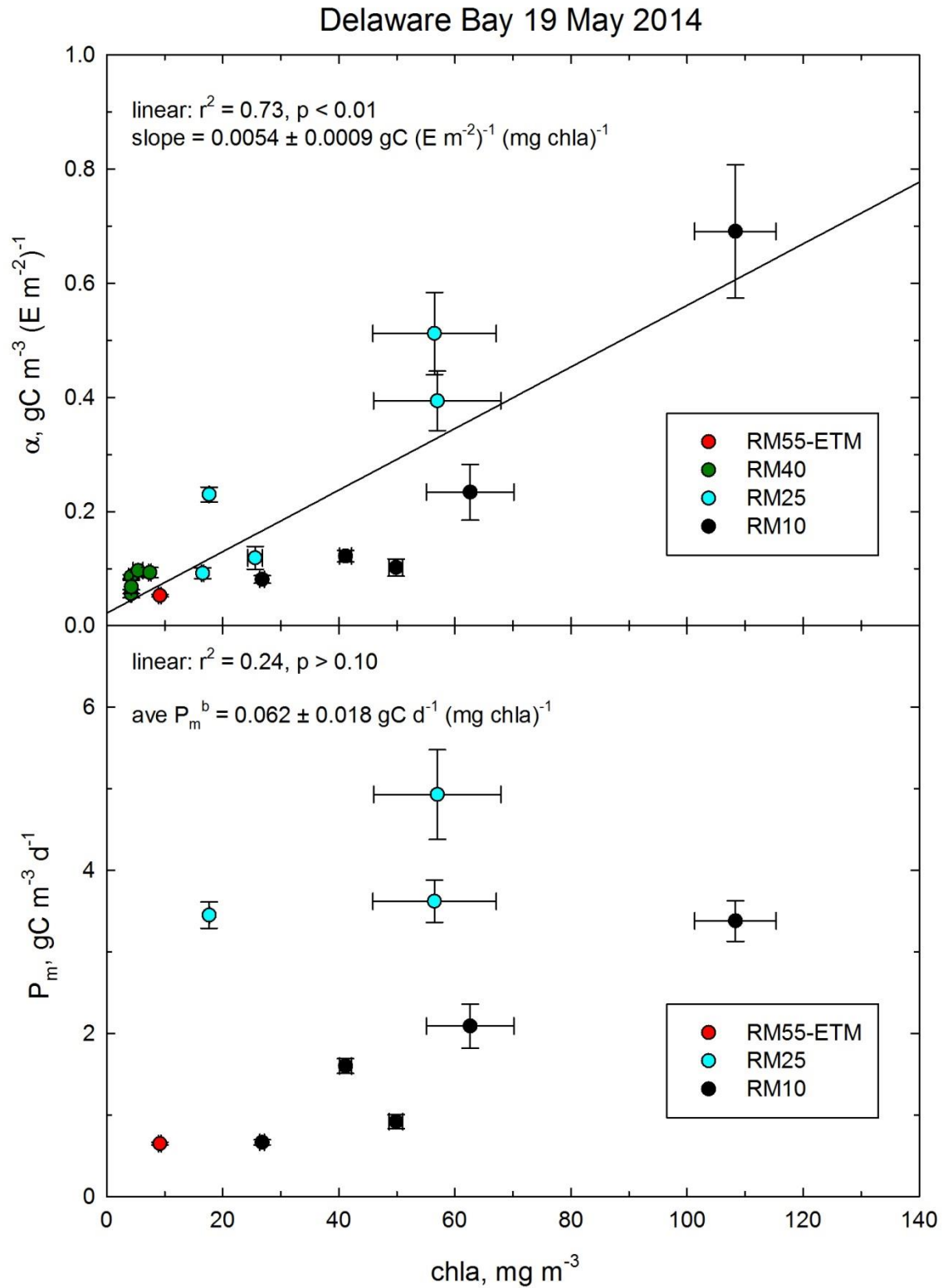
Figure 7A. Relationship between the photosynthetic parameters α and P_m to chlorophyll *a* (chla) in May 2014 on river mile stations (RM) in Delaware Bay.
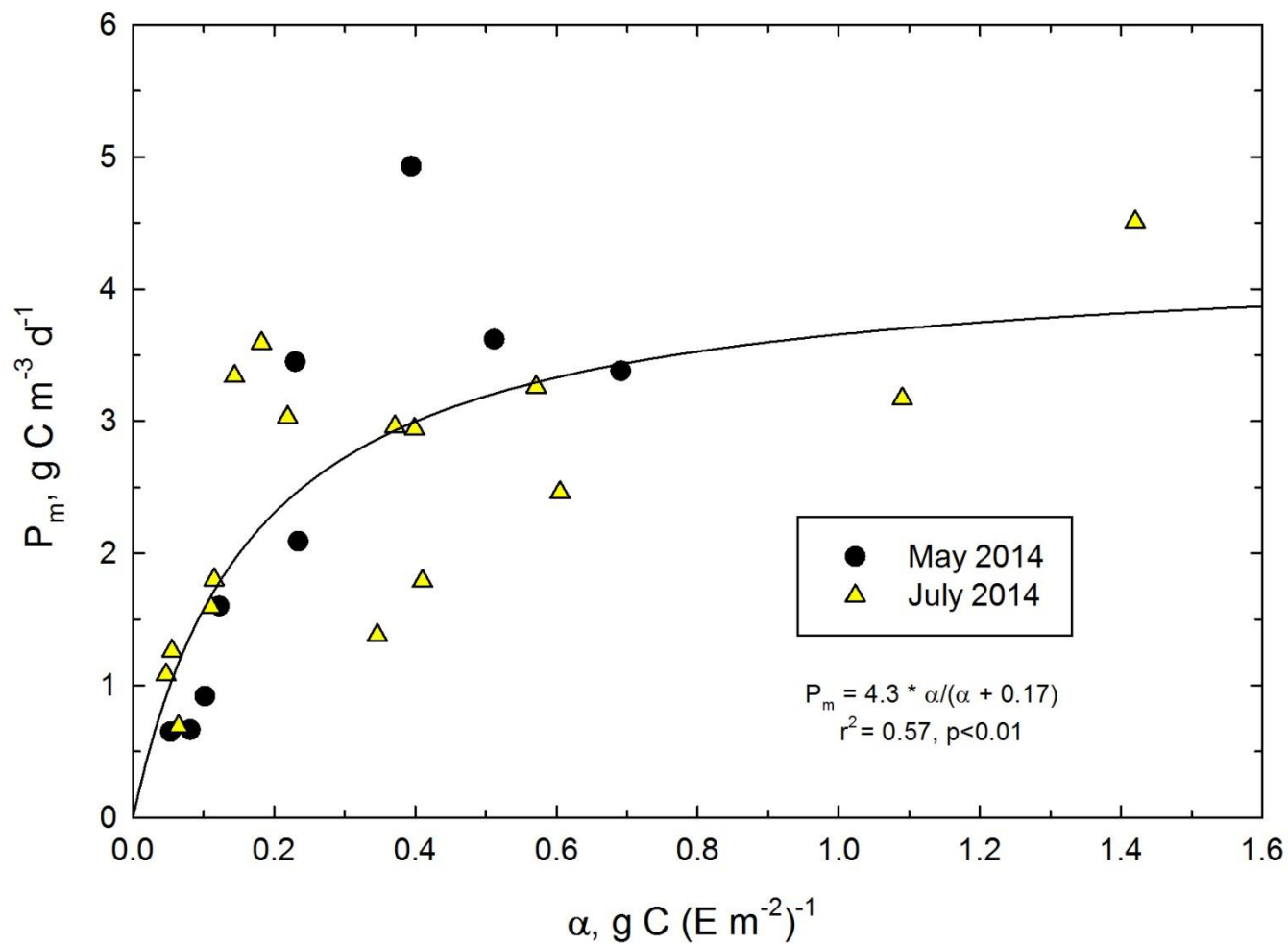
Delaware Bay 21 July 2014

linear: $r^2 = 0.66$, p < 0.01
slope = 0.016 ± 0.003 gC $(E\ m^{-2})^{-1}$ $(mg\ chla)^{-1}$

hyperbola: $r^2 = 0.58$, p < 0.01

Figure 7B. Relationship between the photosynthetic parameters α and P_m to chlorophyll *a* (chla) in July 2014 on river mile stations (RM) in Delaware Bay.

Figure 8. Hyperbolic relationship between the light-independent, maximum rate of C fixation (P_m) and the light-dependent rate of C fixation in Delaware Bay in May and July 2014.
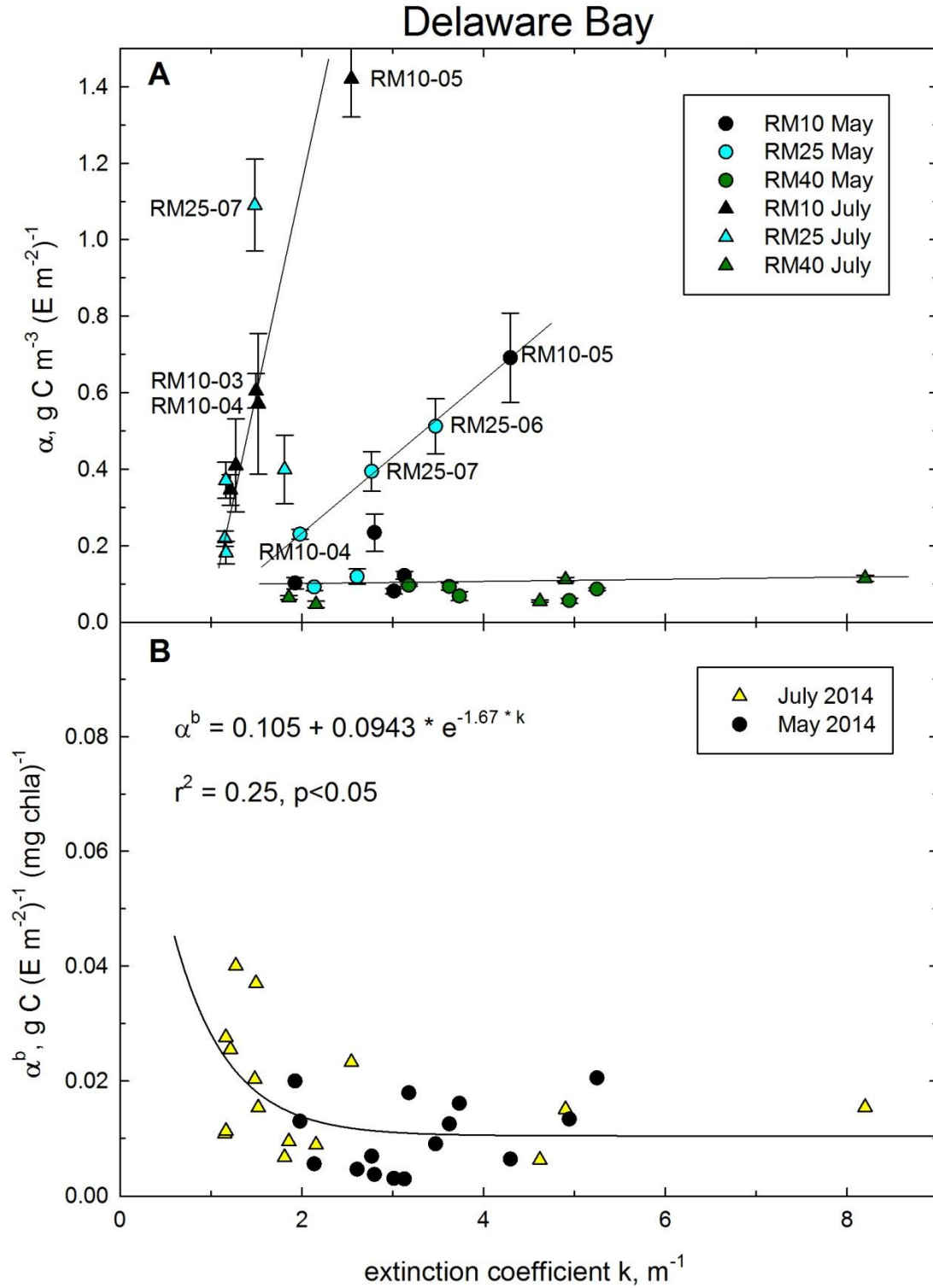
Delaware Bay

Figure 9A. The relationship of the light-dependent photosynthetic parameters α and α^b to the water column extinction coefficient for PAR k. The lines in the upper panel are not statistically fit, but are

approximate groupings by classes of chlorophyll *a*. The effects of chlorophyll a are removed in the lower panel, revealing an exponential relationship between α^b and k for the combined dataset.
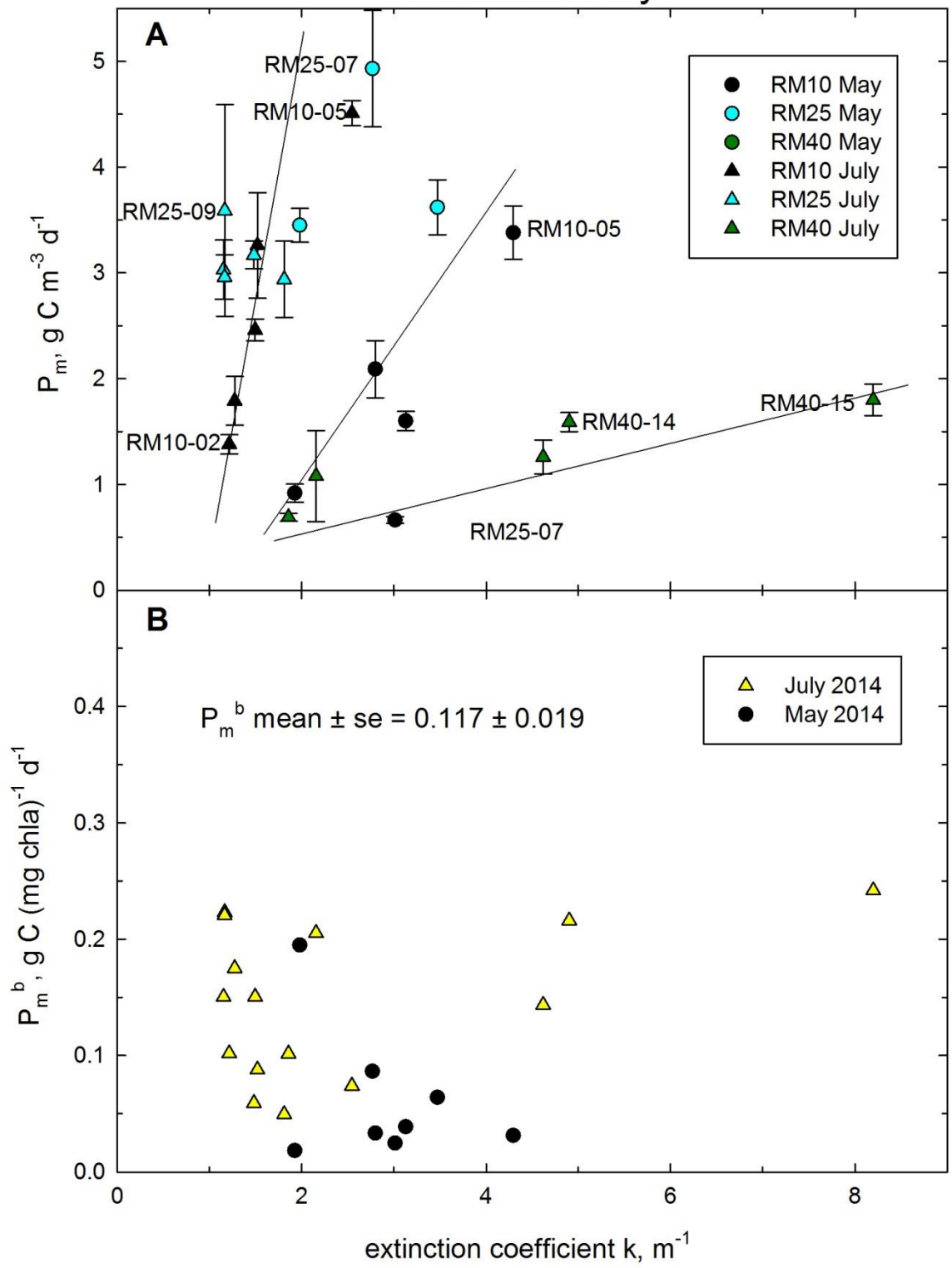
Delaware Bay

Figure 9B. The relationship of the light-saturated photosynthetic parameters P_m and P_m^b to the water column extinction coefficient for PAR (k). The lines in panel A are not statistically fit, but are approximate groupings by classes of chlorophyll *a*. The effects of chlorophyll a are removed in the panel B, revealing no relationship between P_m^b and k for the combined dataset over a narrow range of P_m^b.

Delaware Bay
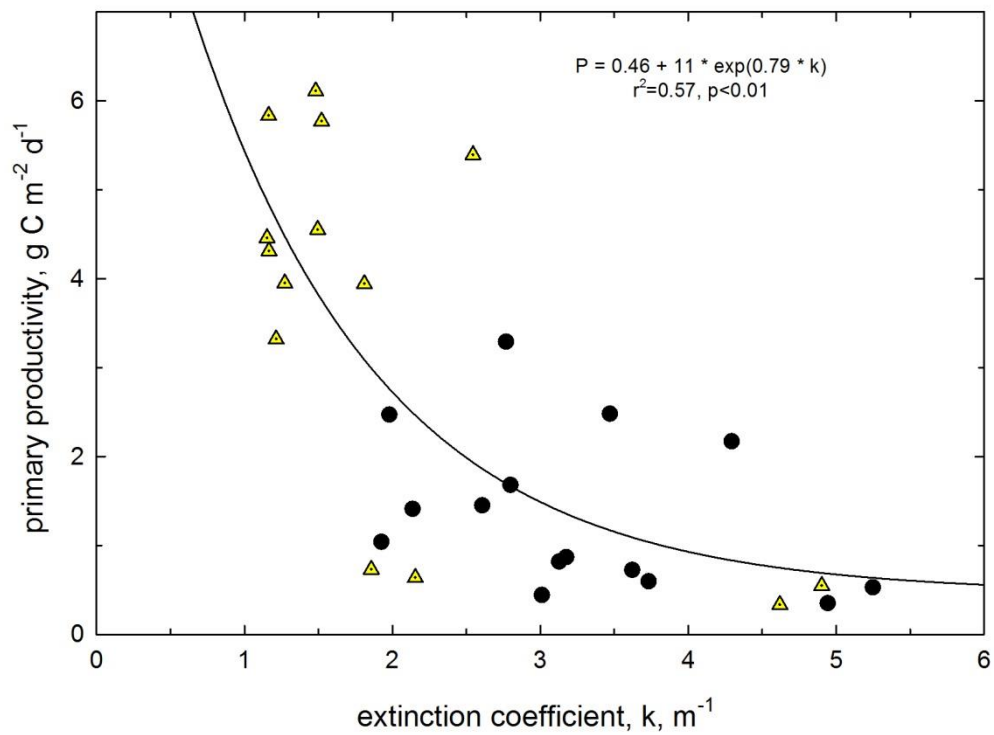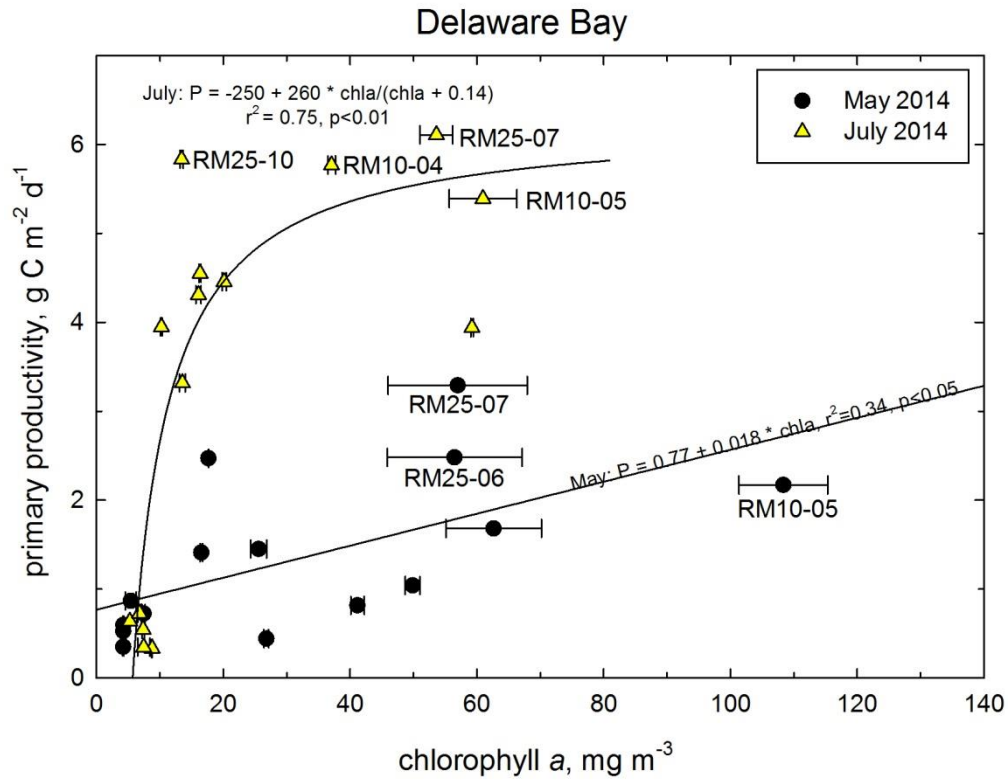
Figure 10. Primary productivity (P) in the water column as a function of surface chlorophyll *a* for May and July 2014 (upper panel), and the relationship of P to the water column extinction coefficient. Compression of

the lighted (euphotic) zone by high k is evident in these data, limiting water column integrated production (P).